J Forensic Sci, May 2005, Vol. 50, No. 3
Paper ID JFS2004223
Available online at: www.astm.org

Min Huang,[1] *Ph.D.; Rachel Russo;*[2] *Barry G. Fookes,*[2] *Ph.D.; and Michael E. Sigman,*[3] *Ph.D.*

Analysis of Fiber Dyes By Liquid Chromatography Mass Spectrometry (LC-MS) with Electrospray Ionization: Discriminating Between Dyes with Indistinguishable UV-Visible Absorption Spectra*

ABSTRACT: Liquid chromatography mass spectrometry (LC-MS) is shown to provide high discriminating power for the identification of textile dyes that can not be reliably distinguished on the basis of their UV/visible absorption profile. Seven pairs of commercial dyes having nearly identical UV/visible absorption profiles and absorption maxima within 5 nm, were identified successfully by LC-MS. Two pairs of cotton fibers, which were indistinguishable by microspectrophotometry, were differentiated by LC-MS. A single wavelength UV/visible detector was used to monitoring dye elution from the column. The utility of the method for comparing questioned and known fibers is discussed.

KEYWORDS: forensic science, fiber dye identification, liquid chromatography mass spectrometry, UV/visible detection

Dye identification and comparison is an important aspect of forensic fiber examination. Currently available methods for dye analysis have limitations for unknown dye identification. Fiber dye extraction protocols provide limited information on dye class; however, specific information on a dye's molecular structure is not obtained by these methods (1). Currently, UV/visible-based approaches to dye analysis involving HPLC with diode array detection or microspectrophotometry are frequently used (2). These methods provide a higher level of discriminating power than simple extraction protocols, but they are unable to differentiate between two structurally similar dyes, i.e. those that differ in structure only by an auxochrome. Liquid chromatography mass spectrometry (LC-MS) has previously been studied as a method of dye analysis (3–16). Of those studies, relatively few have focused on the use of LC-MS or ESI-MS for the analysis of forensic samples or artifacts(3,5,8,16). The use of ESI-MS coupled with collision induced decomposition (CID) has been suggested as a method for the comparison of questioned and known samples, without the use of a chromatographic scheme(3).

In this work, the utility of LC-MS is demonstrated as a method of discriminating between sets of dyes that are indistinguishable by UV/visible spectroscopic methods. The use of LC-MS in the forensic comparison of questioned and known fibers can significantly enhance the analysts' confidence in a common source assertion. Dyes that cannot be discriminated based on UV-visible absorption profile can be distinguished based on mass spectral data. The use of soft ionization techniques, such as the electrospray ionization, can produce ions that retain the dye's molecular structure with little fragmentation. In this case, the mass difference alone can allow the analyst to differentiate between two different dyes that have indistinguishable UV-visible absorption profiles. Molecular fragmentation and MS/MS techniques, as previously demonstrated, (3) can produce additional discriminating information. On the other hand, if dyes extracted from questioned and known items are indistinguishable by UV-visible absorption and mass spectral techniques, the probability of identical dye molecular structure is quite high and a common source assertion can be made with much higher confidence. In cases where the chemical structure of the dye must be elucidated, LC-MS at higher fragmentor voltage settings (>100 V) and LC-MS/MS techniques can provide valuable information to assist in structure determination. The ESI mass spectra for many of the dyes analyzed here have not been previously reported.

Methods

Instrumentation

The mass spectrometer used in this study was an Agilent 1100 MSD quadrupole mass spectrometer equipped with an electrospray ionization (ESI) source and interfaced to an Agilent 1100 HPLC, as previously reported (16). The instrument can be conveniently switched between positive and negative ion modes for the detection of dyes that form either negative or positive ions. Fragment ions can be obtained by changing the "fragmentor" voltage to add additional energy, which induces the decomposition of molecular ions formed in the ESI source. Even at relatively low fragmentor voltages, complex multi-bond fragmentation can be

[1] National Center for Forensic Science, University of Central Florida, P.O. Box 162367, Orlando, FL 32816-2367.
[2] Department of Chemistry, University of Central Florida, P.O. Box 162367, Orlando, FL 32816-2367.
[3] National Center for Forensic Science and Department of Chemistry, University of Central Florida, P.O. Box 162367, Orlando, FL 32816-2367.

* This work was supported under Award number 1998-IJ-CX-K003 from the Office of Justice Programs, National Institute of Justice, Department of Justice. Points of view in this document are those of the authors and do not necessarily represent the official position of the U.S. Department of Justice. The work was done at the National Center for Forensic Science, a National Institute of Justice program hosted by the University of Central Florida, and a member of the Forensic Science Resource Network.

Presented at 56th Annual Meeting of the American Academy of Forensic Sciences, February 16–21, 2004, Dallas TX.

Received 2 June 2004; and in revised form 2 Sept. 2004 and 30 Oct. 2004; accepted 30 Oct. 2004; published 6 April 2005.

observed. The fragmentor voltage is a key parameter in the Agilent 1100 MSD and its optimization for dye analysis has previously been reported (16).

UV-Visible absorption spectra of extracted dyes and dye standards were measured with a Cary-4 spectrophotometer. Spectra were measured for methanol solutions of the dyes in a standard 1 cm path length absorption cell. Background correction was performed using a methanol solvent blank.

HPLC Separation and Mass Spectrometry

Separation was carried out on a ZORBAX Eclipse XDB-C18 (2.1×150 mm) HPLC column at a mobile phase flow rate of 0.20 mL/min. A programmed solvent gradient (methanol/water) was used to achieve better separation. Elution process began at 50% methanol and changed to 95% at 15 min by a steady increase in the methanol composition. The methanol composition was held constant at 95% until the analysis ended at 40 min. Long elution times for each run are necessary to elute all of the co-extracted components and keep the column clean to ensure reproducible performance, even though many of dyes were eluted from the column during the first 20 min. Mass spectrometer parameters were optimized for maximum sensitivity, as previously reported (16). The drying gas for the ESI was held at 12.0 L/min. and the spray chamber temperature was set at 350°C for all analytes, unless otherwise specified. As a generalized method, a dye-containing sample is first analyzed at a low fragmentor voltage to optimize molecular ion detection. A second analysis may be conducted at a higher fragmentor voltage to induce ion fragmentation and enhance structural elucidation. This report focuses on data collected at low fragmentor voltage (e.g., 60 V). The method for extracting the mass spectral peaks for the dye from the background based on the combined use of a UV-visible absorption and the ESI mass spectra has been addressed previously (16).

Methanol (HPLC grade, AlliedSignal Inc., Burdick & Jackson, Muskegon, MI) was used as received. Water was prepared from Barnstead E-pure (Barnstead/Thermolyne, Iowa), with a resistance of 18.2 MΩ cm. All the dye reagents are from Aldrich Chemical Company, Inc. (Milwaukee WI 53255, USA), and Sigma Chemical Co. (P.O. Box 14508, St Louis, MO 63178). Stock solutions of dyestuffs were prepared in 100% methanol at concentration of 50 μg/mL.

Results and Discussion

Comparing UV/Visible and Mass Spectrometry Data for Commercial Dyes

A UV-visible absorption detector is commonly used as the primary detector for HPLC; however, molecular absorption spectra of organic dyes exhibit broad Franck-Condon envelopes and are not highly characteristic of dye structure. Among the hundreds of commercial fiber dyes, there are many examples of dyes that have minor structural differences, i.e., they differ only in a substituent group (auxochromes), and therefore exhibit similar absorption profiles. The seven pairs of common dyestuffs listed in Table 1 were examined by UV/visible spectroscopy and by LC-MS in an attempt to differentiate between the structurally related dyes. The molecular absorption profiles for acid green 25 and 27, solvent red 26 and 27, and basic red 9 and basic violet 14 are shown in Fig. 1*a*–1*c*, as typical examples of the similarities observed between the absorption profiles of the dye pairs listed in Table 1. Not only are the maximum absorption wavelengths very close for the dye-pair spectra, but also the absorption profiles for each pair are nearly indistinguishable. In Fig. 1, one dye component is shown at one half the concentration of the other dye to facilitate a comparison of the spectral profiles. It can be seen from Fig. 1 that for this set of dyes, neither the maximum absorption wavelength nor the absorption profile allow the analyst to discriminate between the two dyes in each set. The optical effects from light scattering by non-dye components, (i.e., delustering agents) and fiber shape further complicate the direct comparison of the dye absorption profiles measured in-situ by microspectrophotometry.

Basic red 9 and basic violet 14 differ in their chemical structure by the replacement of a hydrogen atom by a methyl group, structures shown in Table 1. The absorption spectra for the two dyes are nearly identical, with only a 5 nm difference in their maximum absorption wavelength. The mass spectra for these two dyes, however, are very different, as shown in Fig. 2*a–b*. The ions initially formed by loss of chloride $[M\text{-}Cl]^+$ have m/z ratios of 288 and 302 respectively for basic red 9 and basic violet 14. These two ions alone can be used to differentiate the two dyes, as would be expected based on their molecular structures. Fragment ions from each initially formed ion also differ, although both dyes fragment to give an ion with m/z ratio of 195. The m/z 195 ions formed from the two dyes may reasonably be expected to be identical. Figure 2*c* shows reasonable fragmentation pathways to account for the observed fragments. The formation of the fragment ion with m/z 271 can be accounted for by loss of $\text{-}CH_3$ and $\text{-}NH_2$ groups. The m/z 271 ion likely arises from a secondary fragmentation of the m/z 286 ion; however, MS/MS experiments are required to confirm the m/z 271 formation pathway.

LC-MS has also been used to distinguish disperse red 1 and disperse red 13 with high confidence. Although the UV-visible absorption maximum for these two dyes differ by 14 nm, Table 1, the spectra may be difficult to distinguish in a fiber when measured by microspectrophotometry. Disperse red 1 and disperse red 13 readily form protonated ions at m/z ratios of 315 and 349, respectively, as given in Table 1. These ions dominate the mass spectrum at fragmentor voltage near 60 V and are sufficient to allow the discrimination between two dyes that are not easily distinguishable based on UV-visible spectra. At a fragmentor voltage of nearly 100 V, the dyes decompose to produce spectra containing additional peaks (16).

In another example, acid green 25 and acid green 27 have quite similar chemical structures, differing only in their substitution groups, as shown in Table 1. The former dye has two methyl ($\text{-}CH_3$) groups, while the later has two butyl ($\text{-}CH_2CH_2CH_2CH_3$) groups, leading to a difference of 84 mass units between the two dyes. Nonetheless, these two dyes have indistinguishable molecular absorption profiles with a maximum absorption wavelength at 642 nm for each dye. Under the conditions employed in this study, both dyes form a set of ions that may reasonably be expected to correspond to $(M\text{-}2Na)^{2-}$, $(M\text{-}2Na + H)^-$, $(M\text{-}Na)^-$, $(M\text{-}H)^-$, and $(M + Na\text{-}2H)^-$. Since these ions are derived from differing degrees of deprotonation and sodium ion association of the dye, and do not involve fragmentation of covalent bonds, different ion masses are formed from each dye. The resulting masses are listed in Table 1 and the resulting spectra are shown in Fig. 3. The mass spectra for these two dyes have no common ions and thereby are easily distinguished on this basis.

The dyes acid red 4 and acid red 8 are structurally quite different, Table 1, however, both dyes have maximum absorption wavelengths at 508 nm and are difficult to distinguish based on their UV-visible absorption spectra. These dyes readily form negative ions and are easily discriminated based on mass spectral data. Under the experimental conditions used here, acid red 4 forms an ion with m/z

TABLE 1—*Mass spectral analysis data for the dyes, which are indistinguishable by UV/visible spectroscopy.*

Dye Name	Structure	λ max	Molecular Ions
Dye Pair I			
Acid green 25 M.W. 622	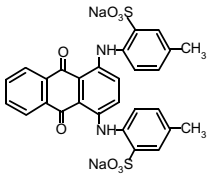	642	288 $[M\text{-}2Na]^{2-}$ 577 $[M\text{-}2Na + H]^{-}$ 599 $[M\text{-}Na]^{-}$ 621 $[M\text{-}H]^{-}$ 643 $[M + Na\text{-}2H]^{-}$
Acid green 27 M.W. 706	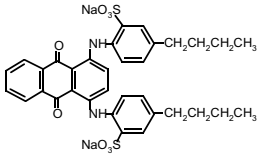	642	330 $[M\text{-}2Na]^{2-}$ 661 $[M\text{-}2Na + H]^{-}$ 683 $[M\text{-}Na]^{-}$ 705 $[M\text{-}H]^{-}$ 727 $[M + Na\text{-}2H]^{-}$
Dye Pair II			
Acid red 4 M.W. 380	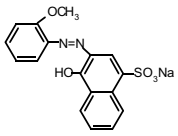	508	357 $[M\text{-}Na]^{-}$
Acid red 8 M.W. 480	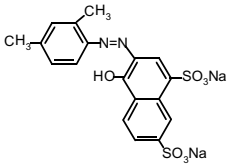	508	217 $[M\text{-}2Na]^{2-}$
Dye Pair III			
Acid red 14 M.W. 502	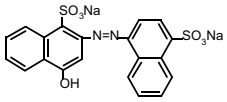	515	228 $[M\text{-}2Na]^{2-}$
Acid red 73 M.W. 556	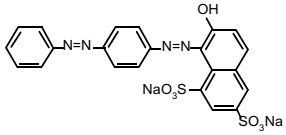	510	255 $[M\text{-}2Na]^{2-}$
Dye Pair IV			
Basic red 9 M.W. 323	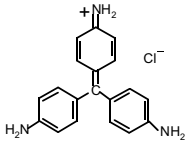	544	288 $[M\text{-}Cl]^{+}$
Basic violet 14 M.W. 337	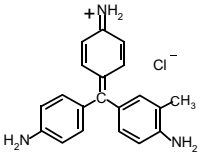	549	302 $[M\text{-}Cl]^{+}$

TABLE 1—*Continued*.

Dye Name	Structure	λ max	Molecular Ions
Dye Pair V			
Disperse blue 3 M.W. 296	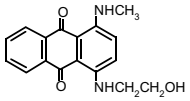	640	319 $[M + Na]^+$ 297 $[M + H]^+$
Disperse blue 14 M.W. 266	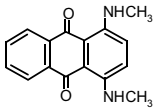	640	267 $[M + H]^+$ 289 $[M + Na]^+$
Dye Pair VI			
Disperse red 1 M.W. 314	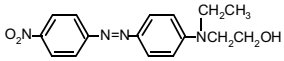	503	315 $[M + H]^+$ 337 $[M + Na]^+$
Disperse red 13 M.W. 348	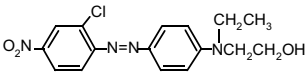	517	349 $[M + H]^+$ 371 $[M + Na]^+$
Dye Pair VII			
Solvent red 26 M.W. 394	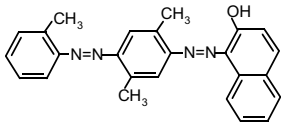	521	393 $[M-H]^-$
Solvent red 27 M.W. 408	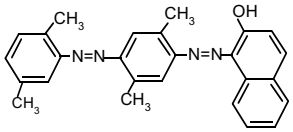	518	407 $[M-H]^-$
Sudan III M.W. 352	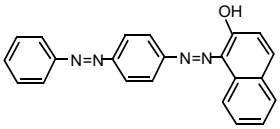	507	351 $[M-H]^-$ 373 $[M + Na-2H]^-$

ratio of 357, reasonably corresponding to $[M-Na]^-$. Acid red 8 forms an ion with m/z ratio 217, which is expected to correspond to $[M-2Na]^{2-}$ (Table 1).

Acid red 14 and acid red 73 also have similar molecular absorption profiles but form very different ions in the mass spectrometer, see Table 1. With two sulfonated sodium salt groups in each dye, they both produce distinguishable negative ions of differing mass by loss of the two sodium atoms. The mass spectrum of acid red 73 contains a dominant $[M-2Na]^{2-}$ ion at an m/z ratio of 255 along with other fragment ions. The m/z 255 ion was previously reported for this dye, along with $[M-2Na + H]^-$ (m/z 511) and $[M-Na]^-$ (m/z 533), (6) which we did not observe. Under our experimental conditions, acid red 14 forms a dominant negative ion at m/z ratio of 228 corresponding to $[M-2Na]^{2-}$. The m/z 228 ion has previously been reported in the LC-ESI-MS analysis of acid red 14, (6) along with $[M-2Na + H]^-$ (m/z 457) and $[M-Na]^-$ (m/z 479), which we did not observe. The formation $[M-xH]^{x-}$ and the sodiated adduct ions have previously been observed for the analysis of polysulphonated anionic dyes by LC-ESI-MS (7).

Disperse blue 3 and disperse blue 14 have similar absorption profiles with maximum UV-visible absorption at 640 nm. The positive ion spectra for the two dyes are displayed in Fig. 4*a–b*. Among other fragments, both spectra contain ions that can reasonably be expected to correspond to $[M + Na]^+$ and $[M + H]^+$, but the two dyes are readily distinguished based the masses of these ions, see Table 1. In this case, both dyes produce ions with a m/z ratio of 252 that may have the same structure, but other ions, including those discussed above, serve to distinguish between the two dyes.

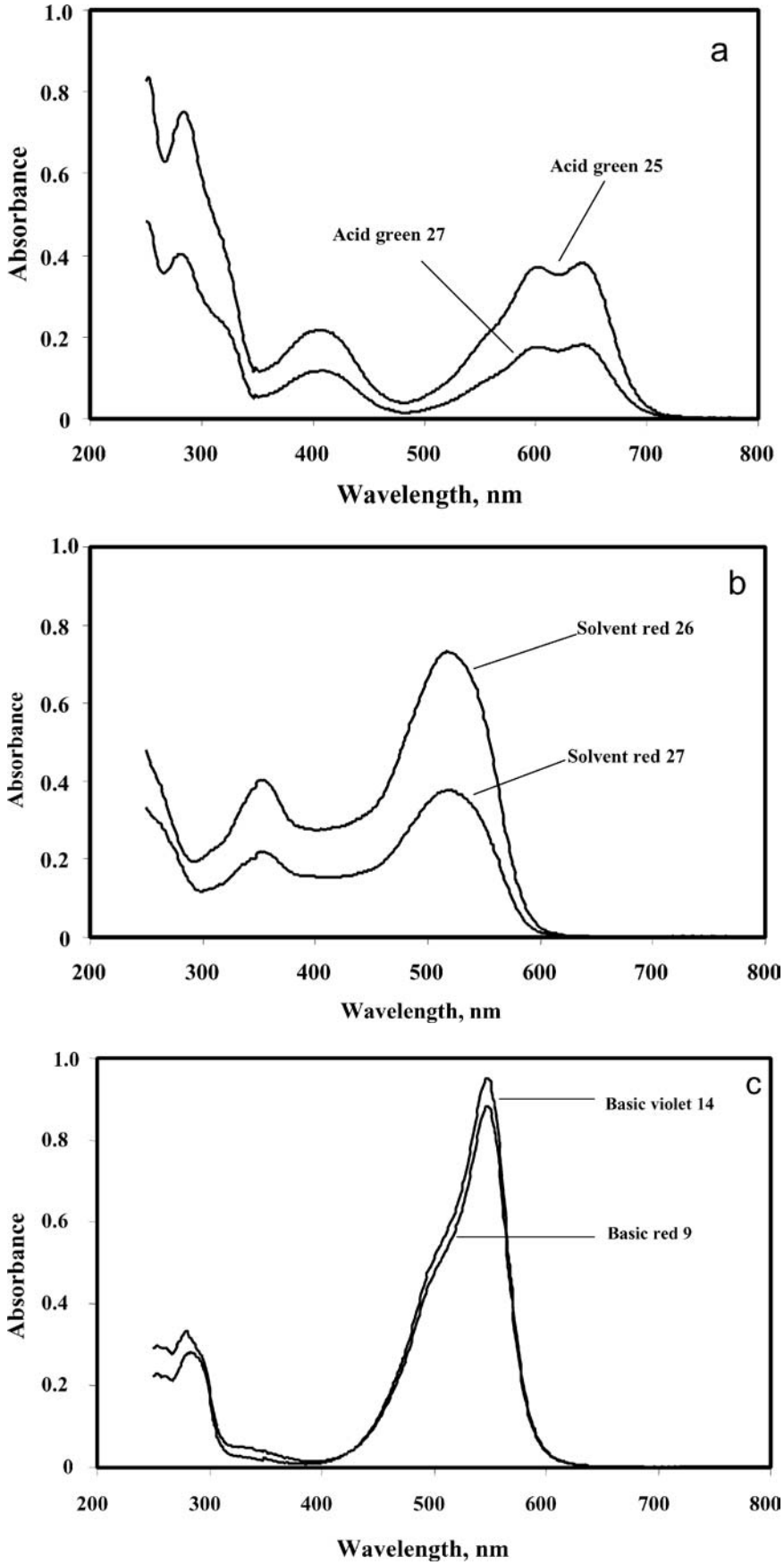

FIG. 1—*(a) Spectra for acid green 25 (10 ppm) and acid green 27 (5 ppm) in 100% MeOH. The wavelengths for the two peaks are 642, 602 nm and 641, 601 nm, respectively. (b) Spectra for solvent red 26 (10 ppm) and solvent red 27 (5 ppm) in 100% MeOH. The maximum absorption wavelengths are the same, 518 nm, for the two dyes. (c) Spectra for basic violet 14 and basic red 9 at concentration of 5 ppm in 100% MeOH. The two dyes have the same maximum wavelength, 548 nm.*

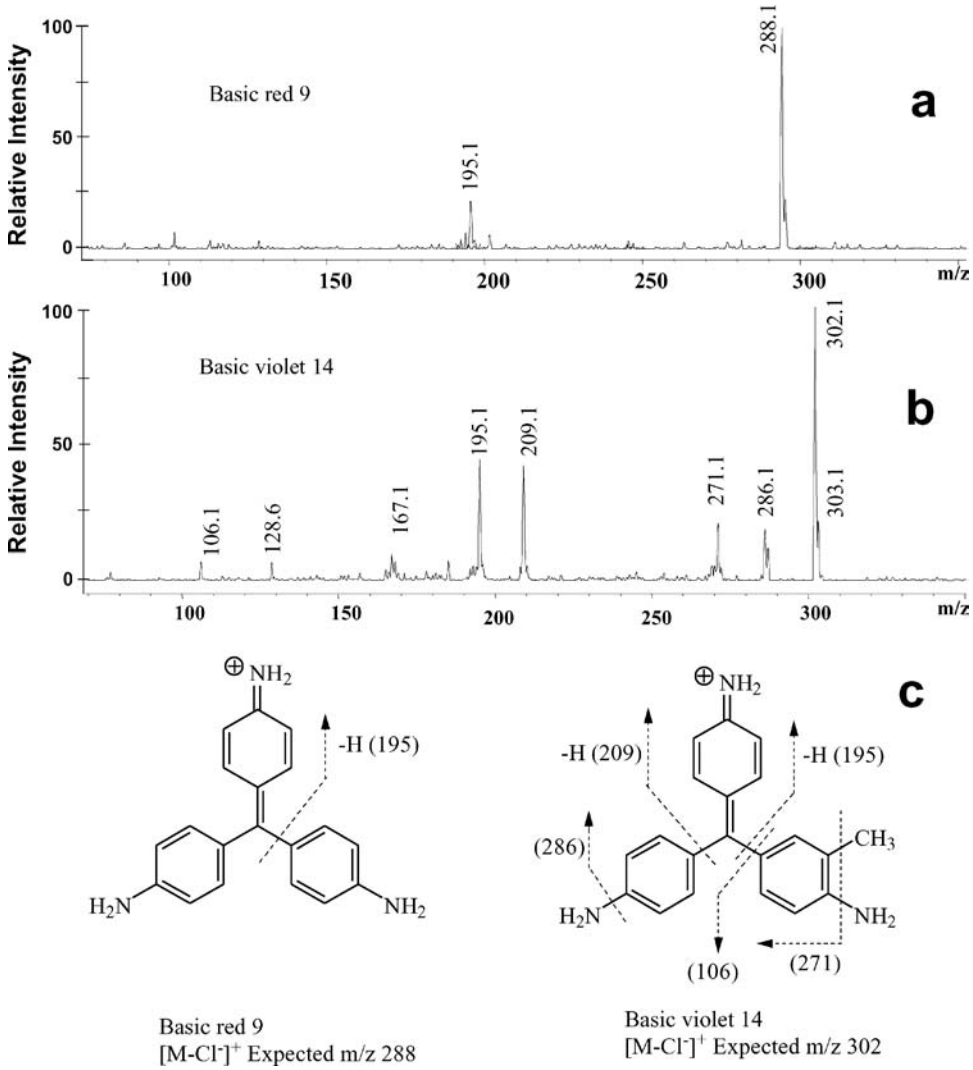

FIG. 2—*(a) ESI (+) mass spectrum of basic red 9. (b) ESI (+) mass spectrum of basic violet 14. (c) Fragmentation pathways expected to lead to the observed ions for basic red 9 and basic violet 14.*

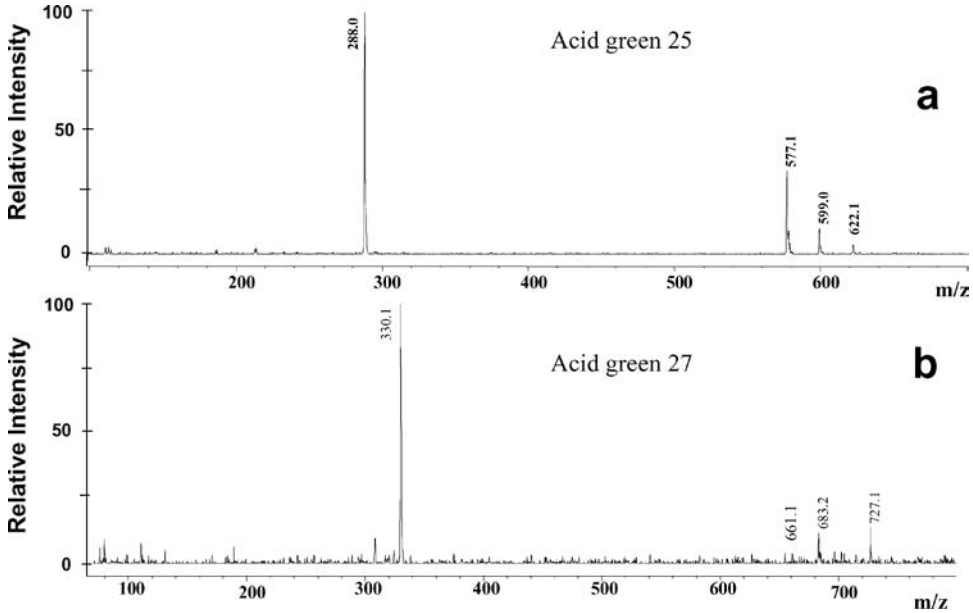

FIG. 3—*(a) ESI (−) mass spectrum of acid green 25. (b) ESI (−) mass spectrum of acid green 27.*

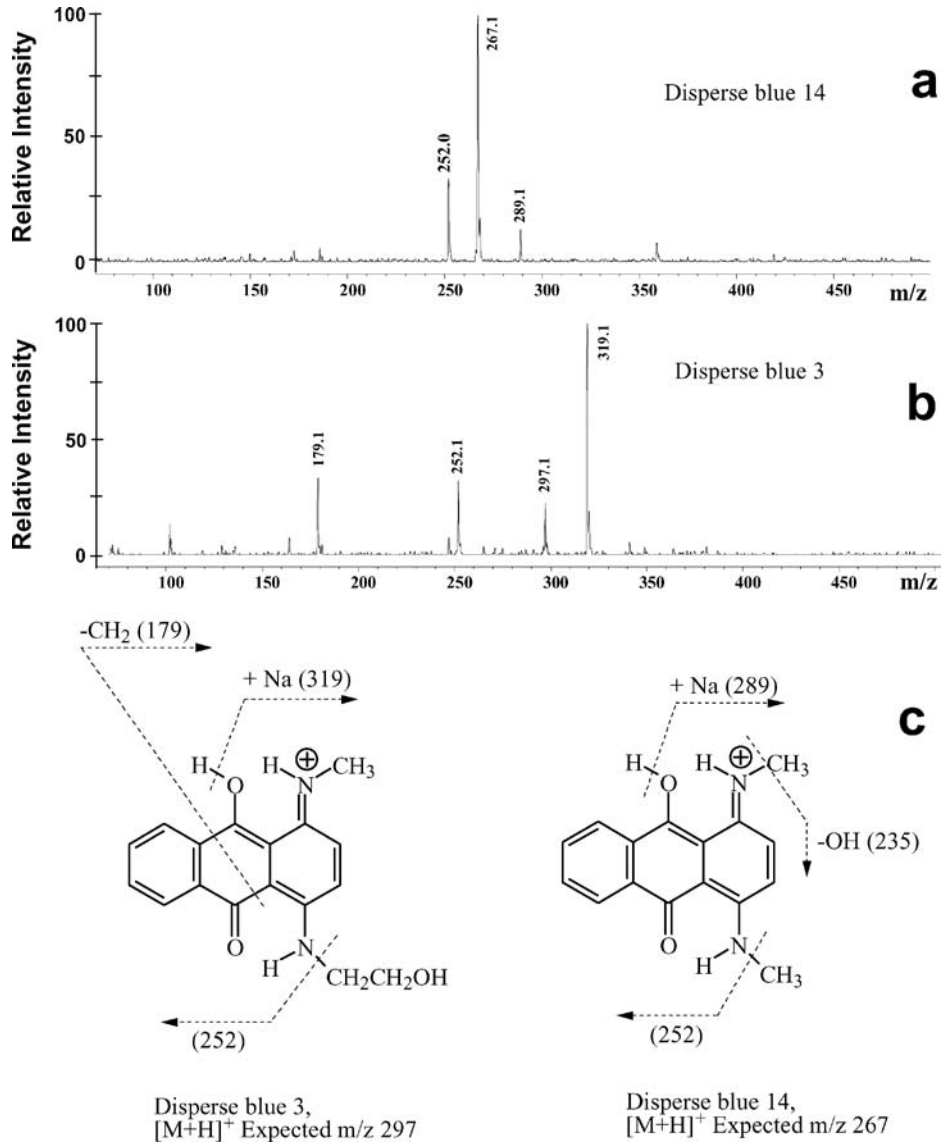

FIG. 4—*(a) ESI (+) mass spectra of disperse blue 3. (b) ESI (+) mass spectrum of disperse blue 14. (c) Fragmentation pathways expected to lead to the observed ions for disperse blue 3 and disperse blue 14.*

Reasonable fragmentation routes are shown in Fig. 4*c* to account for the major ions observed in the spectra. The m/z 179 ion formed from disperse blue 3 can reasonably be accounted for as arising from a complex multi-bond fragmentation occurring across two sigma bonds in the central ring coupled with the additional loss of $-CH_2$.

Solvent red 26 and solvent red 27 also have very similar molecular structures, differing by a single methyl group, as shown in Table 1. These two dyes also have very similar UV-visible absorption profiles and UV-visible absorption maxima that differ by only 3 nm. In the negative ion mode, the expected ions, $[M\text{-}H]^-$, for solvent red 26 and solvent red 27 correspond to different m/z ratios of 393 and 407, respectively, and therefore allow a comparative differentiation between the dyes.

Discriminating Between Extracted Dyes

The seven pairs of dyes discussed above are very difficult to distinguish by UV-visible absorption spectroscopy, and similar challenges can occur with forensic fiber samples. In order to examine the potential for encountering fibers that can not be discriminated based on microspectrophotometry, a set of ten "red" cotton items of highly similar color were purchased. The items included cloth remnants/garments and heavy-weight threads. Single fibers from these items were indistinguishable based on appearance under microscopic examination. Of the items, three pairs were found to possess indistinguishable absorption profiles and absorption maxima by microspectrophotometry. The fibers from one pair were distinguished based on the extraction behavior of their dyes following FBI-SWGMAT protocols (1). The fibers from a second pair were distinguished based on the behavior of their dyes in the mass spectrometer. One dye produced ions only under positive polarization, and the other dye produced ions only under negative polarization, allowing discrimination between the fibers, although the chromatographic behaviors of the two dyes were highly similar. In the third case, the dyes from the two fibers both produced ions under negative polarity in the ESI; however, the mass spectra were readily distinguishable, as shown in Fig. 5, thus eliminating a common source. Figure 6 shows the similarity of the

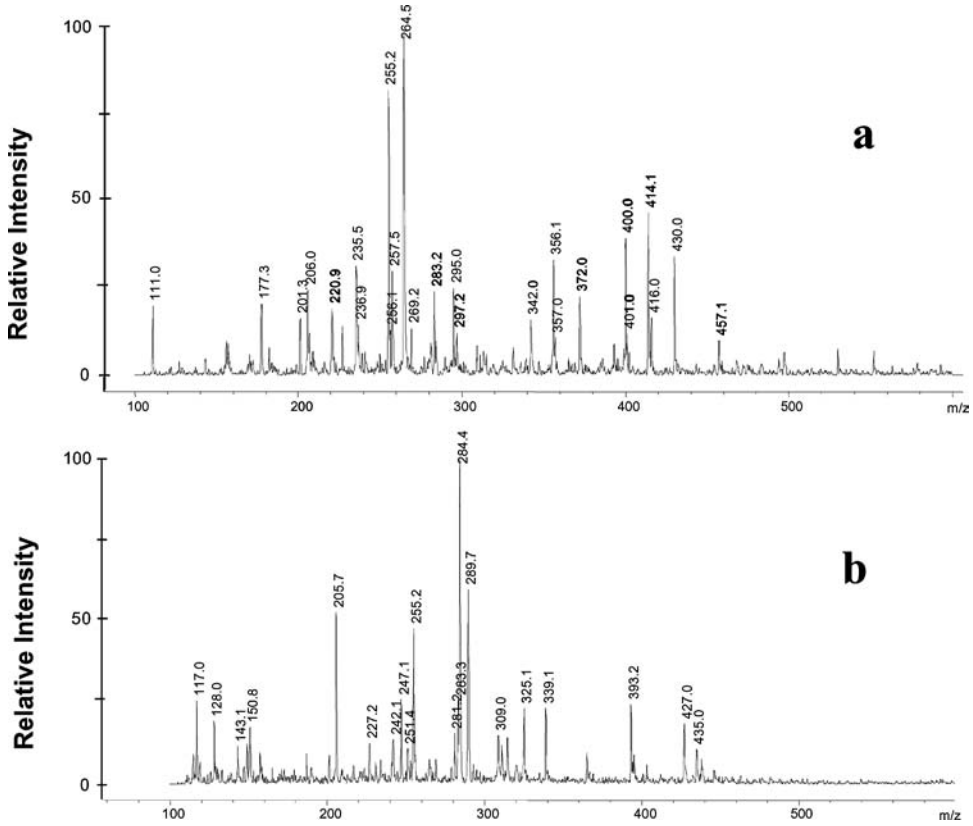

FIG. 5—*Mass spectra obtained by ESI under negative polarity for dyes extracted from two red cotton fibers, which were indistinguishable by microspectrospectophotometry.*

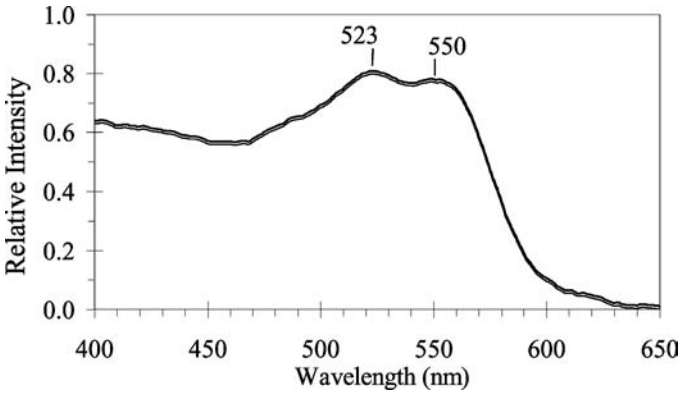

FIG. 6—*UV-visible spectra measured by microspectrophotometry for two red cotton fibers. The corresponding mass spectra are shown in Fig. 5.*

microspectrophotometry data for the extracted dyes that produced the mass spectra shown in Fig. 5.

The examples given here demonstrate the potential of LC-MS for discriminating between known and questioned fibers where the dyes are different at the molecular level. When LC-MS fails to differentiate between two fibers based on their dye content, it is recommended that the analysis be extended to include LC-MS/MS or MS/MS of the extracted dye mixture as previously reported (3).

Acknowledgments

This work was supported under Award number 1998-IJ-CX-K003 from the Office of Justice Programs, National Institute of Justice, Department of Justice. Points of view in this document are those of the authors and do not necessarily represent the official position of the U.S. Department of Justice. The work was done at the National Center for Forensic Science, a National Institute of Justice program hosted by the University of Central Florida, and a member of the Forensic Science Resource Network.

References

1. Federal Bureau of Investigation, Scientific Working Group on Materials Analysis. Forensic fiber examination guidelines. Forensic Science Communications 1999;1(1): Available at http://www.fbi.gov/hq/lab/fsc/backissu/april1999/houcktoc.htm.
2. Eyring MB. Spectromicrography and colorimetry: Sample and instrumental effects. Anal Chim Acta 1994;288:25–34.
3. Tuinman AA, Lewis LA, Lewis SA Sr. Trace-fiber color discrimination by electrospray ionization mass spectrometry: A tool for the analysis of dyes extracted from submillimeter nylon fibers. Anal Chem 2003;75:2753–60. [PubMed]
4. Bruins AP, Weidolf LOG, Henion JD, Budde WL. Determination of sulfonated azo dyes by liquid chromatography/atmospheric pressure ionization mass spectrometry. Anal Chem 1987;59:2647–52.
5. Yinon J, Saar J. Analysis of dyes extracted from textile fibers by thermospray high-performance liquid chromatography—mass spectrometry. J Chromatogr 1991;586:73–84.
6. Ràfols C, Barceló D. Determination of mono- and disulphonated azo dyes by liquid chromatography–atmospheric pressure ionization mass spectrometry. J Chromatogr 1997;777:177–92.
7. Holčapek M, Jandera P, Přikyl J. Analysis of sulphonated dyes and intermediates by electrospray mass spectrometry. Dyes and Pigments 1999;43:127–37.
8. Novotná P, Pacáková V, Bosáková Z, Štulík K. High-performance liquid chromatographic determination of some anthraquinone and naphthoquinone dyes occurring in historical textiles. J Chromatogr A 1999;863:235–41. [PubMed]

9. Lemr K, Holčapek M, Jandera P, Lyčka A. Analysis of metal complex azo dyes by high-performance liquid chromatography/electrospray ionization mass spectrometry and multistage mass spectrometry. Rapid Commun Mass Spec 2000;14:1881–8.
10. Socher G, Nussbaum R, Rissler K, Lankmayr E. Analysis of sulfonated compounds by ion-exchange high-performance liquid chromatography—mass spectrometry. J Chromatogr A 2001;912:53–60. [PubMed]
11. Holčapek M, Jandera P, Zderadička P. High performance liquid chromatography—mass spectrometric analysis of sulphonated dyes and intermediates. J Chromatogr A 2001;926:175–86. [PubMed]
12. Mayer M, Friel A, Kesners P. Determination of sensitizing disperse dyes by HPLC/MS analysis. GIT Spezial Chromatogr 1998;18:65–66, 68–69.
13. Mayer M, Kesners P, Mandel F. Determination of carcinogenic azo-dyes by HPLC/MS analysis. GIT Spezial Chromatogr 1998;18:20–3.
14. Straub R, Voyksner, RD, Keever JT. Thermospray, particle beam and electrospray liquid chromatography—mass spectrometry of azo dyes. J Chromatogr 1992;627:173–86.
15. Lin H-Y, Voyksner RD. Determination of environmental contaminants using an electrospray interface combined with an ion trap mass spectrometer. Anal Chem 1993:65:451–6.
16. Huang M, Yinon J, Sigman M. Forensic identification of dyes extracted from textile fibers by liquid chromatography mass spectrometry (LC-MS). J Forensic Sci 2004;49(2):238–49. [PubMed]
17. Kiyonami R. Technology of ion-trap type LC-MS system. J Mass Spec Soc Japan 2000;48:202–6.
18. Baumann C, Cintora MA, Eichler M, Lifante E, Cooke M, Przyborowska A, et al. A library of atmospheric pressure ionization daughter ion mass spectra based on wideband excitation in an ion trap mass spectrometer. Rapid Commun Mass Spec 2000;14:349–56.

Additional information and reprint requests:
Michael E. Sigman, Ph.D.
Associate Professor
Department of Chemistry and National Center for Forensic Science
University of Central Florida
P.O. Box 162367
Orlando FL, 32816-2367
E-mail: msigman@mail.ucf.edu